Neurobiology of Learning and Memory 166 (2019) 107070

Contents lists available at ScienceDirect

Neurobiology of Learning and Memory

journal homepage: www.elsevier.com/locate/ynlme

The role of CaMKII-Tiam1 complex on learning and memory

Hiroto Kojima[a,b,c], Morgane Rosendale[b,c,1], Yui Sugiyama[b], Mariko Hayashi[d], Yoko Horiguchi[d], Toru Yoshihara[d], Yuji Ikegaya[a], Takeo Saneyoshi[b,c,*], Yasunori Hayashi[b,c,*]

[a] Laboratory of Chemical Pharmacology, Graduate School of Pharmaceutical Sciences, The University of Tokyo, 7-3-1 Hongo Bunkyo-ku, Tokyo 113-0033, Japan
[b] Department of Pharmacology, Graduate School of Medicine, Kyoto University, Kyoto 606-8501, Japan
[c] RIKEN Brain Science Institute, Wako, Saitama 351-0198, Japan
[d] Institute of Laboratory Animals, Graduate School of Medicine, Kyoto University, Kyoto 606-8501, Japan

ARTICLE INFO

Keywords:
Reciprocally activating kinase-effector complex
Synaptic plasticity
Ca^{2+}/calmodlin-dependent protein kinase II
Actin
Guanine-nucleotide exchange factor
Behaviour battery

ABSTRACT

A stimulation inducing long-term potentiation (LTP) of synaptic transmission induces a persistent expansion of dendritic spines, a phenomenon known as structural LTP (sLTP). We previously proposed that the formation of a reciprocally activating kinase-effector complex (RAKEC) between CaMKII and Tiam1, an activator of the small G-protein Rac1, locks CaMKII into an active conformation, which in turn maintains the phosphorylation status of Tiam1. This makes Rac1 persistently active, specifically in the stimulated spine. To understand the significance of the CaMKII-Tiam1 RAKEC *in vivo*, we generated a Tiam1 mutant knock-in mouse line in which critical residues for CaMKII binding were mutated into alanines. We confirmed the central role of this interaction on sLTP by observing that KI mice showed reduced Rac1 activity, had smaller spines and a diminished sLTP as compared to their wild-type littermates. Moreover, behavioral tests showed that the novel object recognition memory of these animals was impaired. We thus propose that the CaMKII-Tiam1 interaction regulates spine morphology *in vivo* and is required for memory storage.

1. Introduction

A high frequency stimulation of presynaptic fibers causes a transient influx of Ca^{2+} into the postsynaptic compartment, which triggers a series of biochemical reactions that leads to a long-term potentiation (LTP) of synaptic transmissions. At the same time, dendritic spines enlarge, an observation that has been named “structural LTP” (sLTP) (Bosch & Hayashi, 2012; Matsuzaki, Honkura, Ellis-Davies, & Kasai, 2004; Okamoto, Nagai, Miyawaki, & Hayashi, 2004). Actin is the major cytoskeletal element found in dendritic spines. During sLTP, the equilibrium between filamentous (F-) and globular (G-) actin shifts towards F-actin and maintained in the spine (Matsuzaki et al., 2004; Okamoto et al., 2004), suggestive of the presence of an active and persistent mechanism to modify the equilibrium. Rac1, a member of the Rho family of small GTPase proteins, is a good candidate for this regulation. Indeed, a FRET-based sensor shows persistent activation of Rac1 in stimulated spine (Hedrick et al., 2016; Saneyoshi et al., 2019). Also, pharmacological blockade of Rac1 activity during the maintenance phase reverses the spine enlargement to baseline levels (Saneyoshi et al., 2019). Then there must be a mechanism to convert a transient Ca^{2+} signal into persistent Rac1 activity maintained throughout the period of sLTP.

We previously found that activated Ca^{2+}/calmodulin-dependent protein kinase II (CaMKII) persistently interacts with Tiam1, a Rac1-specific guanine nucleotide exchange factor (RacGEF), in stimulated spines (Saneyoshi et al., 2019). The interaction occurs between the “pseudo-autoinhibitory” domain of Tiam1 and the binding pocket “T-site” of CaMKII, normally occupied by the autoinhibitory domain of the kinase. Tiam1 binding to the T-site interrupts the autoinhibition of the kinase such that it becomes persistently activated, which, in turn, causes a persistent phosphorylation of Tiam1, even after Ca^{2+} concentration subsides. This mechanism can therefore convert transient Ca^{2+}-signaling into a persistent activation of Rac1 and its downstream actin regulators. Based on this observation, we proposed the concept of a “reciprocally activating kinase-effector complex” (RAKEC) (Saneyoshi et al., 2019). In this work, we explore how the RAKEC-mediated regulation of Tiam1 is related to learning and memory in intact animals. To do so, we generated *tiam1* knock-in (KI) mice harboring mutations in the pseudo-autoinhibitory domain of the Tiam1 protein. We found that KI mice displayed reduced Rac1 activity and that their hippocampal CA1 neurons harbored smaller spines. In addition, their object recognition memory was impaired seven days after training. We conclude

* Corresponding authors at: Department of Pharmacology, Graduate School of Medicine, Kyoto University, Kyoto 606-8501, Japan.
E-mail addresses: saneyoshi.takeo.3v@kyoto-u.ac.jp (T. Saneyoshi), yhayashi-tky@umin.ac.jp (Y. Hayashi).
[1] Current address: University of Bordeaux, 33000 Bordeaux, France.

https://doi.org/10.1016/j.nlm.2019.107070
Received 25 June 2019; Received in revised form 7 August 2019; Accepted 20 August 2019
Available online 21 August 2019

that the CaMKII-Tiam1 interaction is required for normal long-term memory storage.

2. Material and methods

2.1. KI animals

Animal experiments were performed in accordance with the institutional guidelines of RIKEN, Kyoto University, and University of Tokyo.

To generate KI animal with the CRISPR/Cas9 genome editing technology, a web tool (https://benchling.com) was used to design four sgRNAs targeted against the vicinity of the mutation site with high on-target and low off-target effects. We co-transfected each of them in a pX330 vector together with Cas9 and mouse Tiam1 cDNA into HEK293T cells and tested for reduced expression of Tiam1 by immunoblotting. The most effective sequence was sgRNA #1 5′-AGAGC CCGAGTTGCCCC-3′. Other sgRNAs, #2 5′-CCCCCGTTGATGCCC GAG-3′, #3 5′-GCCCTCTCGGGCATCAAC-3′, and #4 5′-GGCCCTCTCG GGCATCAA-3′ were less effective. Approximately 2 pl per egg of mixture of sgRNA #1 (50 ng/μl), Cas9 mRNA (100 ng/μl) and Tiam1 1552–1554 AAA single stranded oligodeoxynucleotide (25 ng/μl for nuclear injection, 100 ng/μl for nuclear + cytosolic or cytosolic injection) was then injected into cytoplasm, nuclei or both of the fertilized eggs from C57BL/6J mice by the RIKEN Research Resource Center core facility. The single-strand oligodeoxynucleotide had the following sequence: 5′- AGACCTTCAGGAGCAGCTTCAGGCTGCCTCCATCAGTCAG CGGGCCCGAGGCCGGAGAACCCTCGATAGCCACGCCTCCCGCATGACA CAGGCCGCGGCGCAAGCGGCACTCTCGGGCATCAACGGGGGCCT GGA-3′. The PAM sequence was modified from CCC to CAC in the single-strand oligodeoxynucleotide sequence to prevent Cas9 from cutting after successful editing.

For genotyping, tail biopsy specimens (~5 mm) were incubated for 10 min at 95–100 °C with 120 μl of 50 mM NaOH, neutralized with 80 μl of 1 M Tris-HCl (pH 8.0) and centrifuged to remove debris. The supernatant was used as a template for PCR. PCR conditions were as follows: 94 °C for 2 min, 40 × [94 °C for 20 s, 60 °C for 30 s, 72 °C for 30 s], 72 °C for 2 min. The following primers, designed by primer BLAST, were used for genotyping: Forward primer 5′-CTGCCCCAAGC AAGTCTCTT-3′, Reverse primer for mutant 5′-GTGCCGCTTGCGCCG-3′, Reverse primer for wild-type 5′-AGGGCCGCTTGCTTCTTG-3′. The primer for the sequencing of Tiam1 genome was 5′-GTACGAGGAGCA GGATGACA-3′. We backcrossed the homozygous KI mice with WT C57BL/6J mice twice and used one of heterozygous mice to expand the colony.

For behavior experiments, male 8–12-week old mice were housed under controlled temperature and humidity on a 12:12-h light/dark cycle with the lights on from 7:00 a.m. to 7:00 p.m., and had access to food and water *ad libitum*. The tests were performed between 9:00 a.m. and 6:00 p.m. The age of animals when behavior tests were performed is summarized in Table 1.

2.2. Reagents and plasmid constructs

Tris-buffered saline (TBS) contained 137 mM NaCl, 2.7 mM KCl, 25 mM Tris-HCl (pH 7.5); TBS-T: TBS with 0.05% (v/v) Tween 20. DDM lysis buffer: 0.1% *n*-dodecyl-β-D-maltopyranoside (DDM, Dojindo), 150 mM NaCl, 50 mM Tris-HCl (pH 8.5), 10% glycerol, 10 mM glycerophosphate, 1 mM Na_3VO_4, 10 mM $MgCl_2$, and 0.2 mM $CaCl_2$. BOS lysis buffer: 1% (w/v) NP40, 50 mM Tris-HCl (pH 7.4), 200 mM NaCl, 10% (v/v) glycerol, 0.5 mM β-glycerophosphate, 10 mM $MgCl_2$, and 0.2 mM $CaCl_2$. IP wash buffer: 20 mM Tris-HCl (pH 8.0), 150 mM NaCl, 0.1% (w/v) DDM, 5% (v/v) glycerol; GST wash buffer: TBS with 1 M NaCl. Complete protease inhibitor cocktail (Roche) and phosphatase inhibitor cocktail (Nacalai tesque) were added to the lysis buffer before use.

The plasmids encoding myc-CaMKIIα and FLAG-Tiam1 were previously described (Saneyoshi et al., 2019). The CaMKII-Tiam1 binding deficient mutant was generated by site-directed mutagenesis using QuikChange Multi Site-Directed Mutagenesis Kit (Agilent Technologies).

Table 1
Summary of tests.

	Animal Age	Figure number
Mouse cohort 1 (n = 12 each)		
Body weight	8–14 weeks	Fig. S1
Rectal temperature	8–14 weeks	Fig. S1
Wire hang tes	8–14 weeks	Fig. S1
Grip strength test	8–14 weeks	Fig. S1
Open field test	9–15 weeks	Fig. S2
Rotor rod test	9–15 weeks	Fig. S3
Y-maze test	9–15 weeks	Fig. S4
Elevated plus maze	9–15 weeks	Fig. S5
Light/dark transition test	9–15 weeks	Fig. S5
Hotplate test	10–16 weeks	Fig. S3
Porsolt forced swim test	10–16 weeks	Fig. S6
Acoustic startle response test	11–17 weeks	Fig. 8
Pre-pulse-inhibition test	11–17 weeks	Fig. 8
Tail suspension test	13–19 weeks	Fig. S6
Mouse cohort 2 (n = 12 each)		
Novel object recognition test, 1 day	8–11 weeks	Fig. 7
Mouse cohort 3 (n = 12 each)		
Novel object recognition test, 7 days	8–11 weeks	Fig. 7

Name of tests and age of animals when the tests were conducted are shown.

2.3. Antibodies

Anti-Tiam1 rabbit antibody (C-16 and N-15, for western blotting), anti-β-actin monoclonal antibody (C-4), anti-Homer 1b/c monoclonal antibody (D-8) and anti-PSD-95 monoclonal antibody (7E3) were obtained from Santa Cruz Biotechnology; anti-β-PIX rabbit antibody (#4515), anti-cofilin1 rabbit antibody (#3318), and anti-Pak1 rabbit antibody (#2602) from Cell Signaling; anti-CaMKII monoclonal antibody (clone 45), anti-Rac1 monoclonal antibody (clone 102), and anti-LIMK1 monoclonal antibody (clone 42) from BD Bioscience; anti-GluA1 rabbit antibody (ab31232) and anti-NeuN rabbit antibody (ab177487) from Abcam; anti-GluN2B monoclonal antibody (MAB5778) and anti-Kalirin rabbit antibody (07-122) from Millipore, anti-Tiam1 sheep antibody (for immunoprecipitation) from R&D Systems; anti-mouse IgG HRP-linked whole antibody and anti-rabbit IgG HRP-linked whole antibody from GE healthcare. Anti-mouse IgG Alexa Fluor 488 or anti-rabbit IgG Alexa Fluor 488, from Thermo Fisher Scientific. For western blotting, the primary antibodies were diluted at 1:1000; the secondary antibodies at 1:5000.

2.4. Immunohistochemistry

The mice were transcardially perfused with 4% (w/v) paraformaldehyde (PFA) in phosphate buffered saline (PBS). The brains were then removed and submerged in 4% PFA at 4 °C for one day. The medium was replaced by PBS and incubated at 4 °C for another day. The vibratome sections (100 μm) were incubated with primary antibodies (1:100) diluted by TNB buffer [0.1 M Tris-HCl (pH 7.5), 0.15 M NaCl, 0.5% blocking reagents (w/v) (Roche)] supplemented with 0.5% Triton-X100 at 4 °C for 1 day. After washing with Tris-buffered (pH 7.5) saline three times, the sections were incubated with Hoechst 33258 (1:1000, Calbiochem), Phalloidin Alexa Fluor 594 (1:200, Thermo Fisher Scientific) and secondary antibodies (1:500, anti-mouse Alexa Fluor 488 or anti-rabbit Alexa Fluor 488) in TNB buffer + 0.5% Triton-X100 at 4 °C for 1 h. After washing with TBS three times, the sections were mounted on cover slips with a drop of mounting media (Vectashield, Vector laboratories). Images were taken by BZ-X700-All-

in-One Fluorescence Microscope (Keyence).

2.5. Golgi-Cox staining

Freshly dissected mouse brains were submerged in Golgi-Cox solution (Zaqout & Kaindl, 2016) for total 7 days in a dark room at room temperature. The medium was replaced by 30% sucrose solution and the brains further incubated at room temperature for 2 days. Then vibratome sections (200 μm) were made and washed twice with deionized water. The precipitation of metallic mercury was performed with 28% ammonia water for 30 min. The sections were dehydrated with an ethanol series (50, 70, 80, 90, and 100%). After cleaning three times with xylene, the sections were left in the solution consisting of 1:1:1 mixture of xylene, chloroform, and ethanol for 2 h in darkness. The slices were mounted on slides with Entellan New (Merck Millipore). The images were taken with 100 × oil immersion objective lens (Olympus).

2.6. Immunoblot analysis, immunoprecipitation, and Pak1 CRIB pull-down assay

For GST pull-down assay, mouse forebrains were homogenized with 9 volumes of the BOS lysis buffer and centrifuged at 100,000 *g* for 1 h to obtain soluble supernatant fraction. One milliliter of the supernatant was subjected to GST-pull down assay with 50 μg of GST-PAK1-CRIB plus 25 μl of glutathione agarose (GST-Accept, Nacalai tesque). For immunoprecipitation, soluble fraction from mouse forebrains was obtained using the DDM lysis buffer. The lysates were immunoprecipitated with 50 μl of Protein G-agarose (IgG-Accept, Nacalai tesque) plus 5 μg of anti-Tiam1 antibody (R&D Systems) or normal goat IgG (Santa Cruz Biotechnology) at 4 °C for 3 h. After washing with the same buffer for 3 times, bound proteins were eluted with 100 μl of 2 × SDS sample buffer. Western blotting was performed as previously described (Saneyoshi et al., 2019).

2.7. Hippocampal slice culture and gene transfection

Hippocampal organotypic slice cultures were prepared from postnatal day 6–7 mice as described (Okamoto et al., 2004). Slices were transfected after DIV 5–7 with a plasmid encoding GFP by ballistic method (Helios Gene Gun System, Bio-Rad).

2.8. Two-photon microscopy imaging and induction of sLTP in single spines

sLTP experiments were carried out with a two-photon microscope (Olympus) with two Ti:sapphire lasers (Sprectra-Physics) in apical dendrites of CA1 pyramidal neurons essentially as described (Bosch et al., 2014).

2.9. Novel object recognition test (NORT)

After handling by the experimenter for a week, mice were placed near a wall of an open field arena (50 × 50 × 50 cm) and allowed to explore for 15 min (Yamasaki et al., 2008). One day later, two identical objects were placed near corners of the arena (5 cm from each adjacent wall) and the mice were again allowed to explore the arena for 15 min. For the test session, the mice were divided into two groups to be tested after 1 or 7 days. On the day of the test, two objects were placed in the same positions as in the training session but one was replaced by a novel object. The mice were allowed to explore the arena for 5 min. Explorative behavior was defined as sniffing or touching the object with nose and/or forepaws. Sitting on the object was not considered as exploration. The memory score was calculated as a discrimination ratio for each mouse with the following formula: (T2 − T1)/(T1 + T2), where T1 = time spent exploring the familiar object and T2 = time spent exploring the novel object.

2.10. Neuromuscular strength

The neuromuscular strength was measured with the grip strength test and wire hang test. A grip strength meter (O'Hara & Co., Tokyo, Japan) was used (Yamasaki et al., 2008).

2.11. Open field test

Each mouse was placed in the center of the open field apparatus (40 × 40 × 30 cm; Accuscan Instruments, Columbus, OH). The spontaneous locomotor activity was measure by the total distance traveled (in cm) and time spent in the center were recorded for 60 min (Belzung & Griebel, 2001; Holmes, 2001; Yamasaki et al., 2008).

2.12. Accelerating rotarod test

Mice were placed on rotating drums (3 cm diameter, UGO Basile Accelerating Rotarod) and the speed of the rotarod accelerated from 4 to 40 rpm over a 5 min period. The time animals could stay on the rod were measured (Yamasaki et al., 2008).

2.13. Hot plate test

Mice were placed on a 55 °C hot plate (Columbus Instruments) and latency to the first hind-paw response, defined as either a paw shake or a paw lick, was recorded (O'Callaghan & Holtzman, 1975; Yamasaki et al., 2008).

2.14. Y-maze test

A Y-shaped maze with three white, opaque plastic arms at a 120° angle from each other was used (Belforte et al., 2010; Le Pen et al., 2006; Yamasaki et al., 2008). After introduction to the center of the maze, mice were allowed to freely explore the maze for 5 min and the number of arm entries was recorded. The percentage of alternation was calculated by: N1/(N2 − 2), where N1 = The number of entry sequences into arms other than the one which the mice had entered just before, for at least three times consecutively, N2 = The total number of entries into any arm.

2.15. Light/dark transition test

The light/dark transition test was performed in a cage (21 × 42 × 25 cm) divided into two sections of equal size by a partition with a passage (O'Hara & Co., Tokyo, Japan) (Cryan & Holmes, 2005; Yamasaki et al., 2008), one brightly illuminated (390 lx) and the other dark (2 lx). Mice were placed into the dark side and allowed to move freely between the two sections for 10 min. The total number of transitions, the time spent on each side, the first latency to enter the bright side as well as the distance traveled were recorded.

2.16. Elevated plus-maze test

The elevated plus-maze (O'Hara & Co., Tokyo, Japan) consisted of two open arms (25 × 5 cm) with 3-mm high plastic ledges and two enclosed arms of the same size with 15-cm high transparent walls (Cryan & Holmes, 2005; Yamasaki et al., 2008). The maze was placed at 55 cm above the floor. Mice were placed in the central square of the maze (5 × 5 cm), facing one of the closed arms and monitored for 10-min. The number of entries into the open and closed arms, the time spent in the open arms (s), and total distance traveled (cm), were recorded.

2.17. Porsolt forced swim test

The Porsolt forced swim test was carried out in a plastic cylinder

(20 cm height × 10 cm diameter) filled with water (23 °C) up to a height of 7.5 cm (Cryan & Holmes, 2005; Yamasaki et al., 2008). The distance traveled during 10 min was monitored.

2.18. Tail suspension test

Mice were suspended 30 cm above the floor in a visually isolated area by adhesive tape placed 1 cm from the tip of the tail, and their behavior was recorded over a 10 min test period (Cryan & Holmes, 2005; Yamasaki et al., 2008).

2.19. Startle response/prepulse inhibition tests

Startle response/prepulse inhibition tests were performed in a startle reflex measurement system (O'Hara & Co., Tokyo, Japan) (Yamasaki et al., 2008). Mice were placed in a plastic cylinder for 10 min. The response to a startle noise (white noise, 40 msec) was recorded for 140 ms starting with the onset of the prepulse stimulus. The background noise level in each chamber was 70 dB. The peak startle amplitude recorded during the 140 ms sampling window was used as the dependent variable. A test session consisted of six trial types (*i.e.* two types for startle stimulus only trials, and four types for prepulse inhibition trials). The intensities of the startle stimulus were 90, 100, 110 or 120 dB. The prepulse sound was presented 100 ms before the startle stimulus, and its intensity was 74 or 78 dB. Four combinations of prepulse and startle stimuli were used (70–120, 75–120, 80–120, and 85–120). Six blocks of the six trial types were presented in pseudorandom order such that each trial type was presented once within a block. The average inter-trial interval was 15 s (range: 10–20 s).

3. Results

3.1. Generation of tiam1 KI mice

We used the CRISPR/Cas9 genome editing technology (Doudna & Charpentier, 2014) to generate *tiam1* KI mice harboring mutations in the CaMKII binding domain of Tiam1 (leucine 1552, lysine 1553, lysine 1554 to alanines (LKK-AAA)) (Saneyoshi et al., 2019) (Fig. 1A). We first designed 4 single guide RNAs (sgRNAs) targeted against the vicinity of the mutation site with high on-target and low off-target effects using a web tool (https://benchling.com) (Fig. 1B). To check their efficacy, we subcloned each sgRNA into a pX330 vector (Cong et al., 2013) and co-transfected them with Cas9 and mouse Tiam1 cDNA into HEK293T cells to analyze the expression level of Tiam1 by immunoblotting. sgRNAs #1 showed the highest efficiency in reducing Tiam1 expression (Fig. 1C) and was thus used for genome editing. sgRNA #1, Cas9 mRNA and single-stranded oligodeoxynucleotides (ssODN) Tiam1 1552–1554 AAA were injected into the cytoplasm, nuclei or both of fertilized eggs. All conditions yielded mutant pups with cytoplasmic injection allowing for the highest viability and efficiency (Supplementary Table S1). From a total of 500 injected eggs, we obtained 69 mutant pups, out of which 19 were heterozygous and 4 homozygous KI. We used one homozygous mouse to further expand the colony after confirming the sequence of the mutation site and the vicinity. KI mice were born at the expected Mendelian ratio and did not show any abnormality in gross appearance, weight, or behavior. Rectal temperature and muscle strength were not significantly different between KI and WT mice (Fig. S1). There was also no obvious difference in brain structure including layer structures between KI and WT (Fig. 2).

We performed immunostaining against Tiam1, finding similarly diffuse expression patterns in WT and KI mouse brain slices (Fig. 2B). We then examined Tiam1 expression levels by western blotting, finding comparable levels in hippocampal homogenates from WT and KI mice (Fig. 3). In addition, the expression levels of representative synaptic proteins were comparable (Fig. 3). The knock-in therefore neither affected basic brain architecture nor synaptic protein expression at this resolution.

We then checked if the CaMKII-Tiam1 interaction was disrupted in KI animals by co-immunoprecipitation from brain tissue of CaMKII and Tiam1 using an anti-Tiam1 antibody. Co-immunoprecipitated CaMKII was significantly lower in KI animal than in WT littermate (Fig. 4A and B), confirming that CaMKII-Tiam1 interaction was impaired in KI mice. Although we only tested for a Tiam1 interaction with the α subunit of CaMKII here, we expect that the KI also affects interaction with the β subunit because critical residues lining T-site, such as F98, E139, I205, and W237 (numbering based on α subunit. Bayer et al., 2006; Saneyoshi et al., 2019) are well conserved among subunits. Since we observed that the CaMKII-Tiam1 complex regulates Rac1 activity *ex*

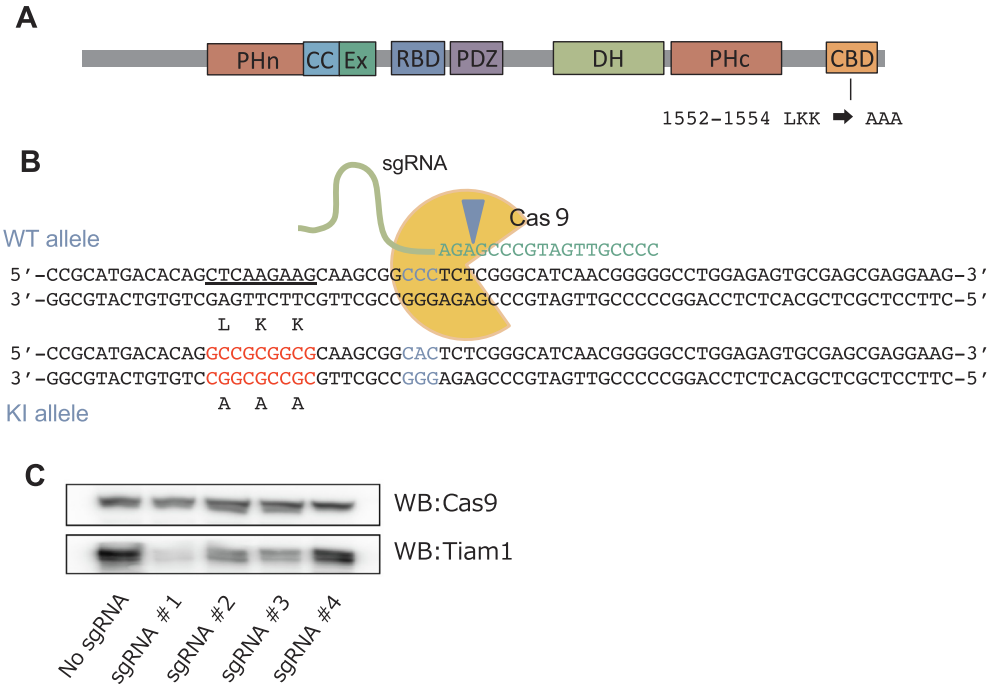

Fig. 1. Design of sgRNAs for genome editing. **(A)** Domain structure of Tiam1 and mutated region on CaMKII binding domain. PHn; N-terminal pleckstrin homology domain, CC-Ex; a coiled-coil region with adjacent sequence, RBD; Ras-binding domain, PDZ; PSD-95/DlgA/ZO-1 domain, DH; catalytic Dbl homology domain, PHc; C-terminal pleckstrin homology domain, CBD; CaMKII binding domain. **(B)** Schema of CRISPR/Cas9 mediated KI. The genomic DNA (top) was digested by Cas9 nuclease and a guide RNA (green) near the CaMKII binding domain of Tiam1. PMA sequence in blue. Blue triangle shows expected cleavage site. The sequence of homologous single stranded oligodeoxynucleotide with KI mutation (red) is also shown. **(C)** Immunoblot analysis of the efficiency of sgRNAs. Four different sgRNA #1 to #4 were designed and cotransfected with Cas9 and Tiam1 cDNA. (For interpretation of the references to colour in this figure legend, the reader is referred to the web version of this article.)

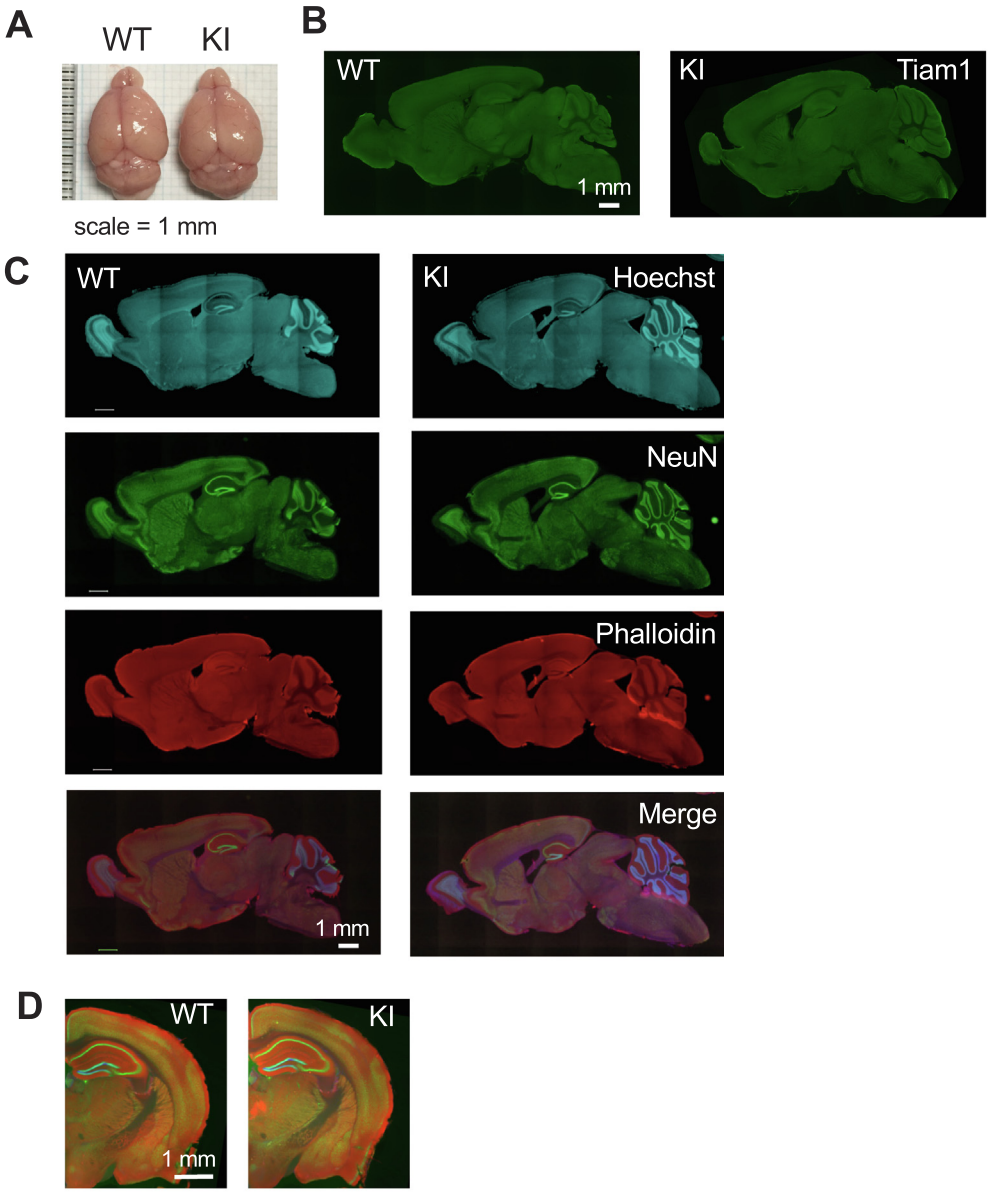

Fig. 2. Brain structure of KI mice is largely unaffected. (A) Macroscopic view of the brains of WT and KI mice. **(B)** Staining with anti-Tiam1 antibody. **(C)** Staining with Hoechst 33258 (blue), anti-NeuN antibody (green), and phalloidine (red). **(D)** Higher magnification of coronal slice showing hippocampus and vicinity, stained similarly to **(C).** (For interpretation of the references to colour in this figure legend, the reader is referred to the web version of this article.)

vivo (Saneyoshi et al., 2019) we checked whether Rac1 activity was affected in KI mice. We used the Pak1 Cdc42/Rac1 interactive binding (CRIB) domain to pull-down active Rac1 or Cdc42 proteins (Saneyoshi et al., 2008). As a result, the KI mice showed significantly lower Rac1 activity compared to their WT littermates (Fig. 4C and D). The activity of Cdc42 was not significantly different between KI and WT, highlighting a selective deficiency. Taken together, these results validate that the CaMKII-Tiam1 interaction is disrupted and that Rac1 activity is dysregulated in KI mice.

3.2. The role of CaMKII-Tiam1 interaction in structural plasticity

Because Tiam1 is important for spine morphogenesis (Tolias et al., 2005, 2007; Zhang & Macara, 2006), the CaMKII-Tiam1 interaction might play a critical role in regulating spine shape during development. We thus first examined by Golgi-Cox staining (Kang et al., 2017; Zaqout & Kaindl, 2016) if basal spine structure was altered in CA1 pyramidal neurons of KI animals (Fig. 5). The density of dendritic spines was comparable to that of WT animals (Fig. 5C). In contrast, spine length and head width were significantly smaller (Fig. 5D).

We then investigated whether the CaMKII-Tiam1 interaction plays a role in plasticity-related spine morphological changes using 2-photon glutamate uncaging (Fig. 6). In neurons of WT mice, dendritic spines enlarged upon stimulation and a measurable size increase was maintained for over 30 min, while unstimulated nearby spines did not show any changes. In contrast, dendritic spines of KI animals did not enlarge in response to glutamate uncaging (Fig. 6B and C). Therefore, we concluded that the CaMKII-Tiam1 interaction is necessary for basal spine morphology and for structural plasticity.

3.3. Behavioral phenotypes of tiam1 KI mice

Because spine morphology and structural spine remodeling are implicated in various behaviors including learning and memory as well as in psychiatric disorders such as anxiety, depression, and autism, we conducted a battery of behavioral tests (Penzes, Cahill, Jones,

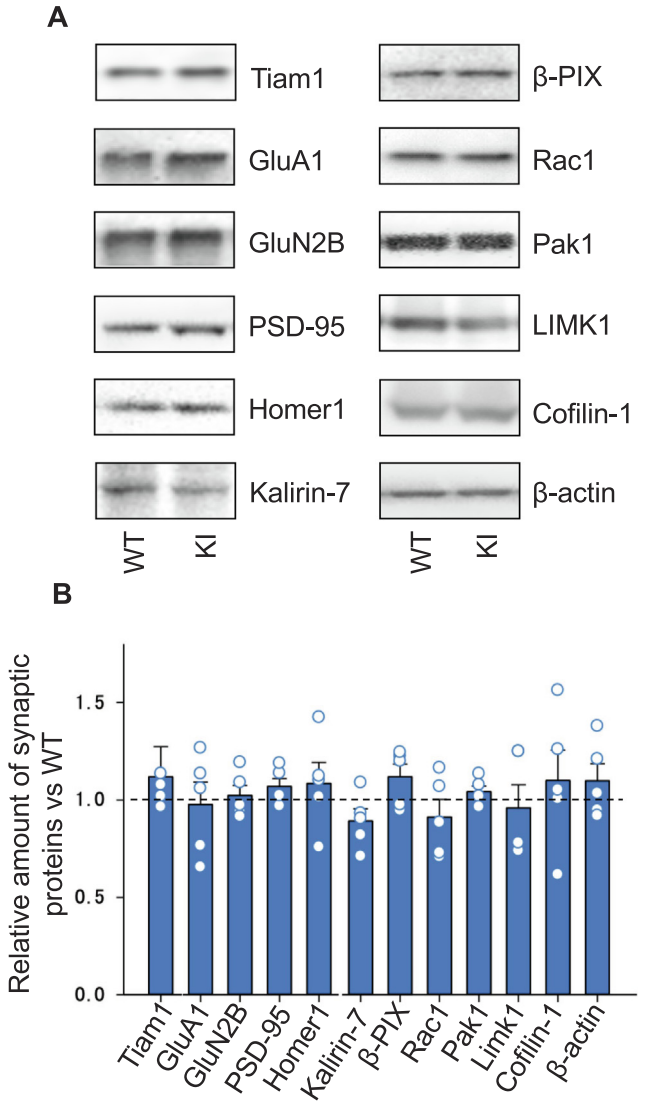

Fig. 3. KI showed comparable expression of synaptic proteins to WT. (A) Western blot analysis of synaptic proteins in hippocampus from KI and WT mice. **(B)** Quantitative analysis of amount of each protein. n = 5 each. Student's *t*-test.

VanLeeuwen, & Woolfrey, 2011; Yamasaki et al., 2008). In open field, hot plate, rotarod, Y-maze, light/dark transition, Porsolt forced swim and tail suspension tests, the KI performed comparably to the WT (Fig. S1–S6, Table 1) indicating overall physical and mental health.

We then more specifically examined learning and memory related functions. For this purpose, we tested a separate cohort of animals on the novel object recognition task (NORT), which requires both the hippocampus and the perirhinal cortex (Antunes & Biala, 2012). Mice were left to explore an arena containing 2 identical objects during a training session before being subjected to a test trial in which one of the objects had been exchanged for a novel one. First, we checked object recognition memory 1 day after training. The memory of the KI mice appeared somewhat poorer than that of their WT littermates but this trend did not reach statistical significance (Fig. 7A). We next examined the performance of a separate group of mice 7 days after training. Under these conditions, KI mice obtained statistically lower memory scores when compared with WT animals (Fig. 7B). These results indicate that CaMKII-Tiam1 dependent sLTP is required for the maintenance of object recognition memory.

Finally, we evaluated the schizophrenia-phenotype of KI mice using a pre-pulse inhibition test (Geyer, Krebs-Thomson, Braff, & Swerdlow, 2001) because abnormal excitatory transmission and plasticity have been related to this disorder. Interestingly, KI mice showed significantly lower pre-pulse inhibition, suggesting a potential implication of the CaMKII-Tiam1 pathway in the pathogenesis of schizophrenia (Fig. 8).

4. Discussions

The necessity of NMDA receptors and CaMKII for LTP as well as for learning and memory is well established (Collingridge, Kehl, & McLennan, 1983; Dhanrajan et al., 2004; Malenka et al., 1989; Malinow, Schulman, & Tsien, 1989; Morris, Anderson, Lynch, & Baudry, 1986; Silva, Paylor, Wehner, & Tonegawa, 1992). However, how these proteins transmit the signal further, eventually causing spine enlargement and increasing AMPA-type glutamate receptor mediated currents is still elusive. The small G-protein of the Rho family Rac1 has been linked to learning and memory *via* several observations. First, Rac1 knock-out induces a significant decrease of learning and memory (Haditsch et al., 2009). Second, Rac1 pharmacological inhibition blocks both electrical and structural LTP (Martinez & Tejada-Simon, 2011; Saneyoshi et al., 2019). Third, Rac1 is persistently activated during sLTP as observed by FRET (Hedrick et al., 2016; Saneyoshi et al., 2019). Given these, it is of great importance to understand the mechanism through which NMDA receptor activation leads to the persistent activation of Rac1 and what the function of persistent Rac1 activation might be.

In this study, we generated a novel KI mouse line disrupting the interaction between CaMKII and the RacGEF Tiam1 by introducing specific point mutations at the CaMKII T-site binding sequence on the carboxyl tail of Tiam1. We confirmed that the CaMKII-Tiam1 interaction regulates the basal activity of Rac1, but not that of Cdc42, a close member of the Rho-family of small G-proteins. We also showed that while the basic brain architecture and synaptic protein composition of KI animals are largely unaltered, there is a significant reduction in the dimensions of hippocampal dendritic spines. The binding between CaMKII and Tiam1 is normally triggered by Ca^{2+} influx through NMDA receptors and persists even after Ca^{2+} levels return to baseline (Saneyoshi et al., 2019). Consistently, in this KI animal, sLTP was impaired. Our results thus indicate that the CaMKII-Tiam1 interaction is necessary for both the maintenance of basal dendritic spine structure and the activity-dependent long-term structural plasticity of dendritic spines. We then went on to test the importance of this interaction in learning and memory and found that KI animals have impaired novel object recognition memory. We indeed observed a trend towards reduced discrimination one day after training and a significant deficit after seven days as compared to their WT littermates. These results are consistent with the idea that sLTP is required for learning and memory, especially during the consolidation phase.

During sLTP, actin filaments are reorganized and polymerized to maintain the enlarged spine structure (Okamoto et al., 2004). As Tiam1 activates Rac1, two downstream pathways may be considered. Activated Rac1 may activate its downstream effectors, the p21-activated kinase (PAK) and the LIM domain containing kinase (LIMK). LIMK would then phosphorylates cofilin1, a key determinant of actin stability and turnover, thereby inhibiting its actin dissociating activity (Arber et al., 1998; Edwards, Sanders, Bokoch, & Gill, 1999; Yang et al., 1998). Alternatively, Rac1 may also activate the WAVE complex and the Arp2/3 complex, which control actin filament branching (Eden, Rohatgi, Podtelejnikov, Mann, & Kirschner, 2002; Miki, Suetsugu, & Takenawa, 1998). Neurons lacking WAVE-1 or the ArpC3 subunit of the Arp2/3 complex, display dendritic spines of abnormal shapes and the Arp2/3 complex is required for sLTP, underlining their importance in the regulation of spine structure (Kim et al., 2013; Soderling et al., 2007). It thus remains to be determined whether CaMKII/Tiam1-activated Rac1 specifically activates either of the cofilin1 or the WAVE/Arp2/3 pathways during LTP and learning.

Tiam1 works not only as a signaling molecule but also as a

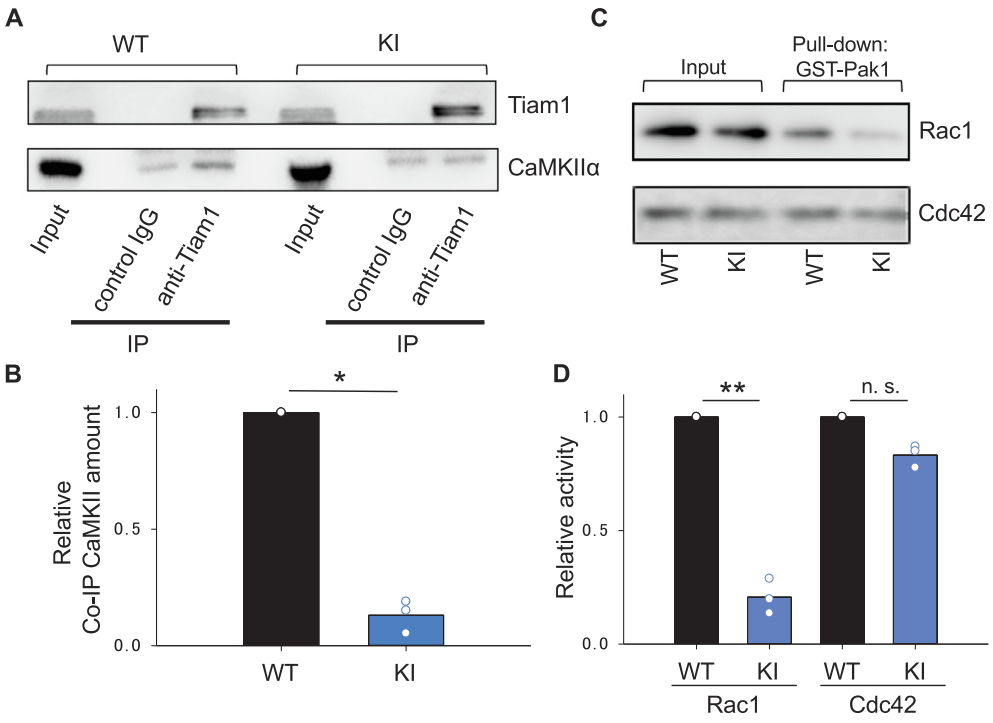

Fig. 4. Interaction between CaMKII and Tiam1 is impaired in KI mice, resulting in reduced Rac activity. (A) Co-immunoprecipitation of CaMKII with Tiam1 using anti-Tiam1 antibody. CaMKII showed a non-specific precipitation with control IgG. This fraction was subtracted as background in the quantification shown in **(B)**. **(B)** Quantitative analysis showed a significant decrease of co-immunoprecipitated CaMKII in KI mice. n = 3. Student's *t*-test, $*p < 0.05$. **(C)** Representative blot of pulled-down of active Rac1 and Cdc42 from KI and WT mice. **(D)** Summary of Rac and Cdc42 activity in KI and WT mice. n = 3 each, Student's *t*-test, $**p < 0.01$.

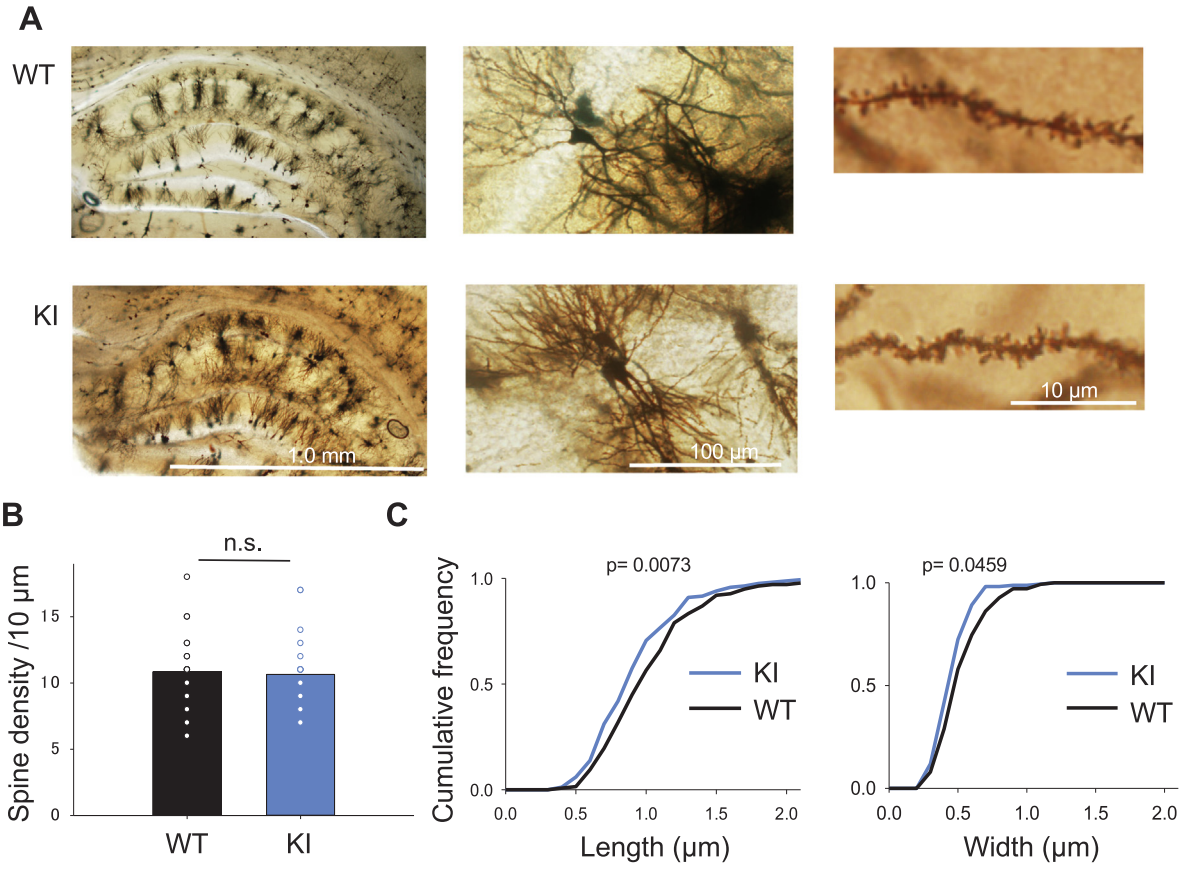

Fig. 5. KI mice had reduced dimensions of spine head. (A) Representative Golgi-Cox staining images of hippocampal CA1 pyramidal neurons from WT and KI mice brains. **(B)** The quantitative analysis of spine density. **C.** Cumulative curves of length and head width of dendritic spines in KI and WT mice Spine numbers: WT, n = 131; KI, n = 167 from each 20 cells. Student's *t*-test, $** p < 0.01$, $* p < 0.05$.

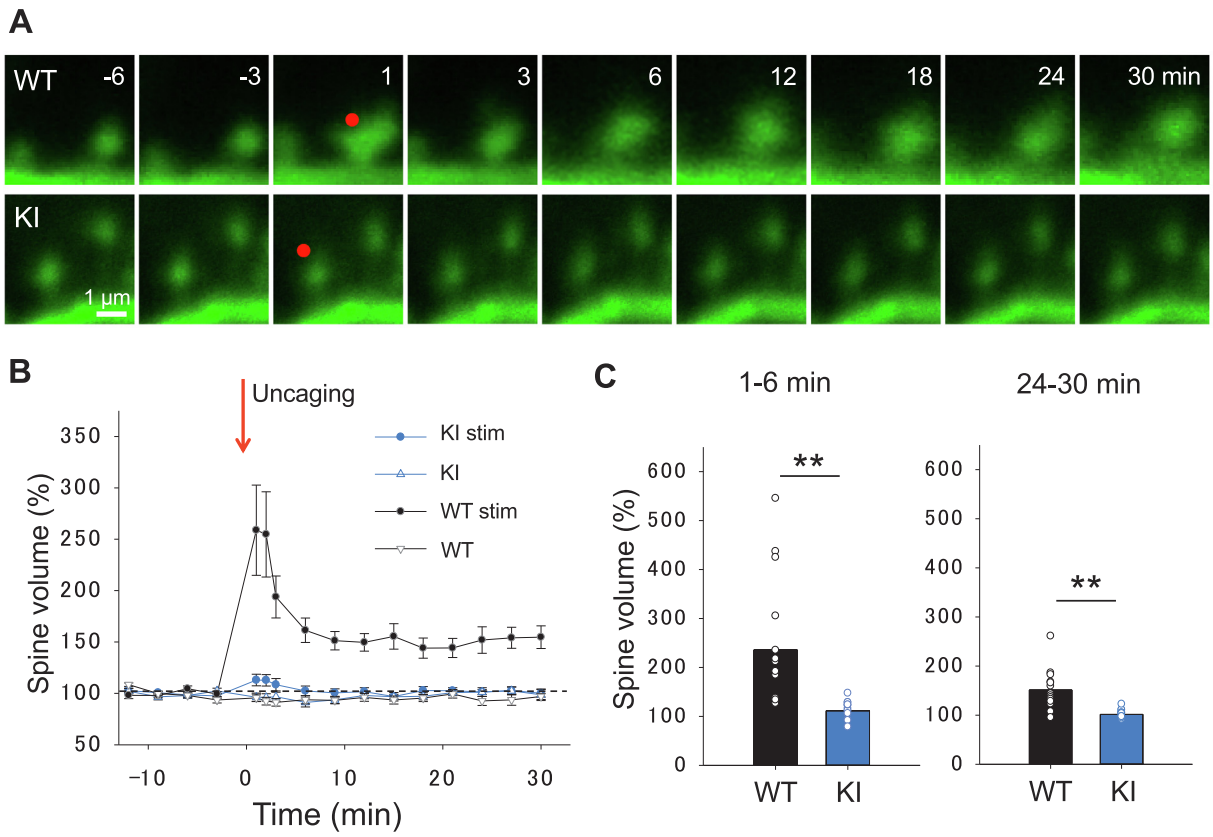

Fig. 6. sLTP was impaired in KI mice. (A) Representative images of glutamate uncaging experiment on single spines. Red dots show stimulated spines. **(B)** Time course of the volume change of each spine. **(C)** The average volume change of spines in transient (1–6 min after stimulation) and sustained phase (24–30 min after stimulation). n = 15 spines. Student's *t*-test, $^{**}p < 0.01$. (For interpretation of the references to colour in this figure legend, the reader is referred to the web version of this article.)

scaffolding molecule for various proteins including NMDA-type glutamate receptor subunit NR1 (Tolias et al., 2005), erythropoietin-producing hematocellular (Eph) receptor (Tolias et al., 2007), spinophilin (Buchsbaum, Connolly, & Feig, 2003) and TrkB, a brain-derived neurotrophic factor (BDNF) receptor (Lai et al., 2012; Miyamoto, Yamauchi, Tanoue, Wu, & Mobley, 2006). Therefore, it is possible that the binding of CaMKII to Tiam1 alters its interaction with these proteins and/or their phosphorylation status.

BDNF stimulates Tiam1 binding to TrkB, which requires S478 phosphorylation through cyclin-dependent kinase 5 (Cdk5). Using TrkB S478A knock-in mice, Lai et al. showed that S478 phosphorylation is required for structural and functional LTP (Lai et al., 2012). In addition, BDNF autocrine activity and TrkB activation are largely dependent on CaMKII during LTP (Harward et al., 2016). The Tiam1-TrkB complex may thus cooperate with the Tiam1-CaMKII RAKEC for the maintenance of LTP. Interestingly, TrkB S478A KI mice showed an impairment in memory consolidation but not in memory acquisition (Lai et al., 2012). This phenotype is similar to the one reported here using Tiam1 mutation KI mice as well as that of dominant-negative PAK transgenic mice (Hayashi et al., 2004). These observations suggest that the CaMKII-Tiam1 RAKEC regulates the memory consolidation process through the TrkB to Pak1 signaling axis.

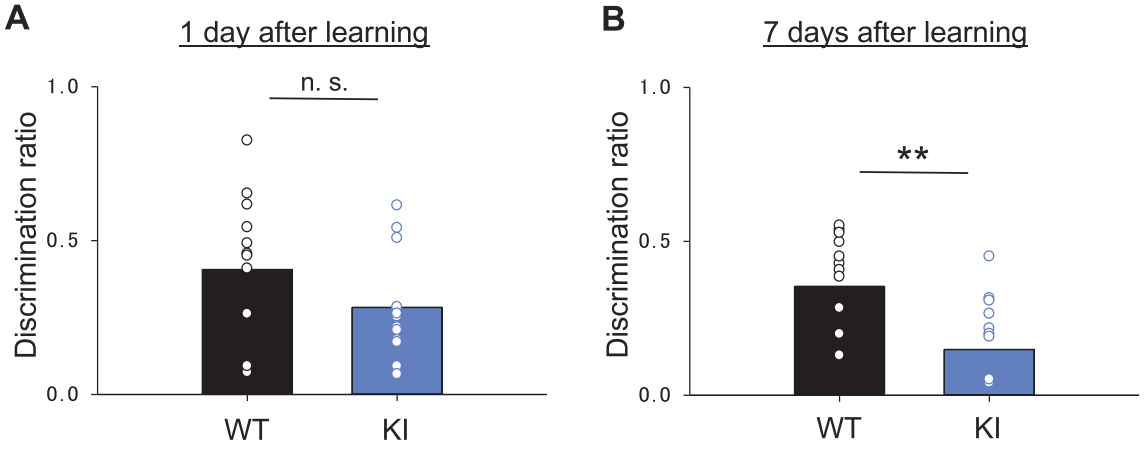

Fig. 7. Impaired novel object recognition test in KI mice. Summary of novel object recognition test 1 (**A**) or 7 (**B**) days after the training session. n = 12 each, Student's *t*-test, $^{**}p < 0.01$.

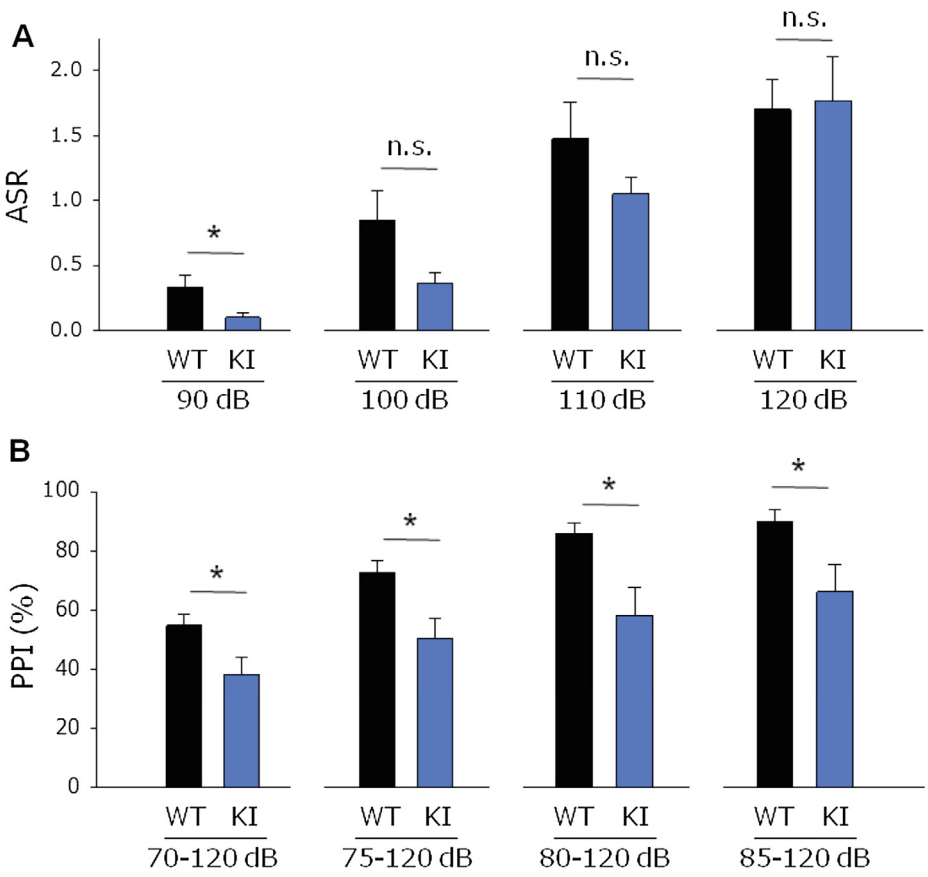

Fig. 8. Reduced pre-pulse inhibition in KI mice. **(A)** The startle response to 90, 100, 110, or 120 dB stimuli. **(B)** A pre-pulse inhibition test for each combination of pre-pulse and startle stimuli (70–120, 75–120, 80–120, and 85–120 dB). n = 12 each, Student's *t*-test, $*p < 0.05$.

Spinophilin also binds Tiam1 and this interaction regulates the actin cytoskeleton (Buchsbaum et al., 2003; Mori et al., 1998). The role of WAVE-1 and spinophilin is not yet fully understood in the context of sLTP, but it is likely that CaMKII signaling also regulates these molecules through Tiam1. Its downstream effector PAK1 has also been implicated in spine structural plasticity and memory (Bosch et al., 2014; Hayashi et al., 2004; Soderling et al., 2003).

On the other hand, the induction of sLTP causes the activation of other Rho-family small GTPases, namely RhoA and Cdc42, in parallel to Rac1 (Murakoshi, Wang, & Yasuda, 2011). In addition, other Rac1-GEFs such as Kalirin-7 and βPIX are required for the structural changes of dendritic spines as well as LTP (Herring & Nicoll, 2016; Saneyoshi et al., 2019). The interplay between the various Rho GTPase pathways, their activators and their effectors may thus be key to encoding various types of memory.

Both hippocampus and perirhinal cortex are required for NORT, though in different aspects (Antunes & Biala, 2012). The perirhinal cortex represents basic information about familiarity or novelty of an object. In contrast, the hippocampus is involved in object memorization by encoding information about the experience of the object (Antunes & Biala, 2012). At this point, it is not clear which brain region caused the impairment in NORT in the KI animals. Tiam1 is widely expressed (Tolias et al., 2005) and likely involved in NMDA receptor-mediated plasticity in various parts of the brain. Therefore, the observed impairment of NORT may be caused either by defective synaptic plasticity in the hippocampus, the perirhinal cortex, or both.

Future studies will be needed to investigate the interplay between synaptic plasticity of individual synapses and memory consolidation as regulated by CaMKII-Tiam1 signaling. It is therefore essential to dissect out the specific involvement of each of these pathways to understand the many aspects of synaptic plasticity, learning and memory.

Declaration of Competing Interest

YH receives research fund from Fujitsu Laboratories and Dwango.

Acknowledgement

HK was recipient of The Junior Research Associate program of RIKEN. MR was a recipient of Long-term Postdoctral Fellowship from JSPS. This work was supported by following agencies: RIKEN, JSPS, Japan (20240032, 16H02455, 22110006, 16F16712, 18H04733, 18H05434 to Y.H.; 24680036, 25113726, 23113522, 18H02528, 18K19377 to T.S.); Human Frontier Science Programme (Y.H.); The Uehara Memorial Foundation (Y.H.); The Naito Foundation (Y.H.); The Takeda Science Foundation (Y.H., T.S.); Japan Foundation for Applied Enzymology (Y.H.); Novartis Foundation (Japan) for the Promotion of Science (Y.H.); Research Foundation for Opto-Science and Technology (Y.H.); Brain Science Foundation, Japan (Y.H.); The Kyoto University Foundation (T.S.), The Shimadzu Science Foundation (T.S.), and The Pharmacological Research Foundation (T.S.).

Appendix A. Supplementary material

Supplementary data to this article can be found online at https://doi.org/10.1016/j.nlm.2019.107070.

References

Antunes, M., & Biala, G. (2012). The novel object recognition memory: Neurobiology, test procedure, and its modifications. *Cognitive Processing, 13*, 93–110.

Arber, S., Barbayannis, F. A., Hanser, H., Schneider, C., Stanyon, C. A., Bernard, O., & Caroni, P. (1998). Regulation of actin dynamics through phosphorylation of cofilin by LIM-kinase. *Nature, 393*, 805–809.

Bayer, K. U., LeBel, E., McDonald, G. L., O'Leary, H., Schulman, H., & De Koninck, P. (2006). Transition from reversible to persistent binding of CaMKII to postsynaptic sites and NR2B. *Journal of Neuroscience, 26*, 1164–1174.
Belforte, J. E., Zsiros, V., Sklar, E. R., Jiang, Z., Yu, G., Li, Y., ... Nakazawa, K. (2010). Postnatal NMDA receptor ablation in corticolimbic interneurons confers schizophrenia-like phenotypes. *Nature Neuroscience, 13*, 76–83.
Belzung, C., & Griebel, G. (2001). Measuring normal and pathological anxiety-like behaviour in mice: A review. *Behavioural Brain Research, 125*, 141–149.
Bosch, M., Castro, J., Saneyoshi, T., Matsuno, H., Sur, M., & Hayashi, Y. (2014). Structural and molecular remodeling of dendritic spine substructures during long-term potentiation. *Neuron, 82*, 444–459.
Bosch, M., & Hayashi, Y. (2012). Structural plasticity of dendritic spines. *Current Opinion in Neurobiology, 22*, 383–388.
Buchsbaum, R. J., Connolly, B. A., & Feig, L. A. (2003). Regulation of p70 S6 kinase by complex formation between the Rac guanine nucleotide exchange factor (Rac-GEF) Tiam1 and the scaffold spinophilin. *Journal of Biological Chemistry, 278*, 18833–18841.
Collingridge, G. L., Kehl, S. J., & McLennan, H. (1983). Excitatory amino acids in synaptic transmission in the Schaffer collateral-commissural pathway of the rat hippocampus. *The Journal of Physiology (London), 334*, 33–46.
Cong, L., Ran, F. A., Cox, D., Lin, S., Barretto, R., Habib, N., ... Zhang, F. (2013). Multiplex genome engineering using CRISPR/Cas systems. *Science, 339*, 819–823.
Cryan, J. F., & Holmes, A. (2005). The ascent of mouse: Advances in modelling human depression and anxiety. *Nature Reviews Drug Discovery, 4*, 775–790.
Dhanrajan, T. M., Lynch, M. A., Kelly, A., Popov, V. I., Rusakov, D. A., & Stewart, M. G. (2004). Expression of long-term potentiation in aged rats involves perforated synapses but dendritic spine branching results from high-frequency stimulation alone. *Hippocampus, 14*, 255–264.
Doudna, J. A., & Charpentier, E. (2014). Genome editing. The new frontier of genome engineering with CRISPR-Cas9. *Science, 346*, 1258096.
Eden, S., Rohatgi, R., Podtelejnikov, A. V., Mann, M., & Kirschner, M. W. (2002). Mechanism of regulation of WAVE1-induced actin nucleation by Rac1 and Nck. *Nature, 418*, 790–793.
Edwards, D. C., Sanders, L. C., Bokoch, G. M., & Gill, G. N. (1999). Activation of LIM-kinase by Pak1 couples Rac/Cdc42 GTPase signalling to actin cytoskeletal dynamics. *Nature Cell Biology, 1*, 253–259.
Geyer, M. A., Krebs-Thomson, K., Braff, D. L., & Swerdlow, N. R. (2001). Pharmacological studies of prepulse inhibition models of sensorimotor gating deficits in schizophrenia: A decade in review. *Psychopharmacology (Berlin), 156*, 117–154.
Haditsch, U., Leone, D. P., Farinelli, M., Chrostek-Grashoff, A., Brakebusch, C., Mansuy, I. M., ... Palmer, T. D. (2009). A central role for the small GTPase Rac1 in hippocampal plasticity and spatial learning and memory. *Molecular and Cellular Neuroscience, 41*, 409–419.
Harward, S. C., Hedrick, N. G., Hall, C. E., Parra-Bueno, P., Milner, T. A., Pan, E., ... McNamara, J. O. (2016). Autocrine BDNF-TrkB signalling within a single dendritic spine. *Nature, 538*, 99–103.
Hayashi, M. L., Choi, S. Y., Rao, B. S., Jung, H. Y., Lee, H. K., Zhang, D., ... Tonegawa, S. (2004). Altered cortical synaptic morphology and impaired memory consolidation in forebrain- specific dominant-negative PAK transgenic mice. *Neuron, 42*, 773–787.
Hedrick, N. G., Harward, S. C., Hall, C. E., Murakoshi, H., McNamara, J. O., & Yasuda, R. (2016). Rho GTPase complementation underlies BDNF-dependent homo- and heterosynaptic plasticity. *Nature, 538*, 104–108.
Herring, B. E., & Nicoll, R. A. (2016). Kalirin and Trio proteins serve critical roles in excitatory synaptic transmission and LTP. *Proceedings of the National Academy of Sciences of the United States of America, 113*, 2264–2269.
Holmes, A. (2001). Targeted gene mutation approaches to the study of anxiety-like behavior in mice. *Neuroscience & Biobehavioral Reviews, 25*, 261–273.
Kang, H. W., Kim, H. K., Moon, B. H., Lee, S. J., Lee, S. J., & Rhyu, I. M. (2017). Comprehensive review of Golgi staining methods for nervous tissue. *Applied Microscopy, 47*, 63–69.
Kim, I. H., Racz, B., Wang, H., Burianek, L., Weinberg, R., Yasuda, R., ... Soderling, S. H. (2013). Disruption of Arp2/3 results in asymmetric structural plasticity of dendritic spines and progressive synaptic and behavioral abnormalities. *Journal of Neuroscience, 33*, 6081–6092.
Lai, K. O., Wong, A. S., Cheung, M. C., Xu, P., Liang, Z., Lok, K. C., ... Ip, N. Y. (2012). TrkB phosphorylation by Cdk5 is required for activity-dependent structural plasticity and spatial memory. *Nature Neuroscience, 15*, 1506–1515.
Le Pen, G., Gourevitch, R., Hazane, F., Hoareau, C., Jay, T. M., & Krebs, M. O. (2006). Peri-pubertal maturation after developmental disturbance: A model for psychosis onset in the rat. *Neuroscience, 143*, 395–405.
Malenka, R. C., Kauer, J. A., Perkel, D. J., Mauk, M. D., Kelly, P. T., Nicoll, R. A., & Waxham, M. N. (1989). An essential role for postsynaptic calmodulin and protein kinase activity in long-term potentiation. *Nature, 340*, 554–557.
Malinow, R., Schulman, H., & Tsien, R. W. (1989). Inhibition of postsynaptic PKC or CaMKII blocks induction but not expression of LTP. *Science, 245*, 862–866.
Martinez, L. A., & Tejada-Simon, M. V. (2011). Pharmacological inactivation of the small GTPase Rac1 impairs long-term plasticity in the mouse hippocampus. *Neuropharmacology, 61*, 305–312.
Matsuzaki, M., Honkura, N., Ellis-Davies, G. C., & Kasai, H. (2004). Structural basis of long-term potentiation in single dendritic spines. *Nature, 429*, 761–766.
Miki, H., Suetsugu, S., & Takenawa, T. (1998). WAVE, a novel WASP-family protein involved in actin reorganization induced by Rac. *EMBO Journal, 17*, 6932–6941.
Miyamoto, Y., Yamauchi, J., Tanoue, A., Wu, C., & Mobley, W. C. (2006). TrkB binds and tyrosine-phosphorylates Tiam1, leading to activation of Rac1 and induction of changes in cellular morphology. *Proceedings of the National Academy of Sciences of the United States of America, 103*, 10444–10449.
Mori, H., Manabe, T., Watanabe, M., Satoh, Y., Suzuki, N., Toki, S., ... Mishina, M. (1998). Role of the carboxy-terminal region of the GluR epsilon2 subunit in synaptic localization of the NMDA receptor channel. *Neuron, 21*, 571–580.
Morris, R. G., Anderson, E., Lynch, G. S., & Baudry, M. (1986). Selective impairment of learning and blockade of long-term potentiation by an N-methyl-D-aspartate receptor antagonist, AP5. *Nature, 319*, 774–776.
Murakoshi, H., Wang, H., & Yasuda, R. (2011). Local, persistent activation of Rho GTPases during plasticity of single dendritic spines. *Nature, 472*, 100–104.
O'Callaghan, J. P., & Holtzman, S. G. (1975). Quantification of the analgesic activity of narcotic antagonists by a modified hot-plate procedure. *Journal of Pharmacology and Experimental Therapeutics, 192*, 497–505.
Okamoto, K., Nagai, T., Miyawaki, A., & Hayashi, Y. (2004). Rapid and persistent modulation of actin dynamics regulates postsynaptic reorganization underlying bidirectional plasticity. *Nature Neuroscience, 7*, 1104–1112.
Penzes, P., Cahill, M. E., Jones, K. A., VanLeeuwen, J. E., & Woolfrey, K. M. (2011). Dendritic spine pathology in neuropsychiatric disorders. *Nature Neuroscience, 14*, 285–293.
Saneyoshi, T., Matsuno, H., Suzuki, A., Murakoshi, H., Hedrick, N. G., Agnello, E., ... Hayashi, Y. (2019). Reciprocal activation within a kinase-effector complex underlying persistence of structural LTP. *Neuron,* 102.
Saneyoshi, T., Wayman, G., Fortin, D., Davare, M., Hoshi, N., Nozaki, N., ... Soderling, T. R. (2008). Activity-dependent synaptogenesis: Regulation by a CaM-kinase kinase/CaM-kinase I/betaPIX signaling complex. *Neuron, 57*, 94–107.
Silva, A. J., Paylor, R., Wehner, J. M., & Tonegawa, S. (1992). Impaired spatial learning in alpha-calcium-calmodulin kinase II mutant mice. *Science, 257*, 206–211.
Soderling, S. H., Guire, E. S., Kaech, S., White, J., Zhang, F., Schutz, K., ... Scott, J. D. (2007). A WAVE-1 and WRP signaling complex regulates spine density, synaptic plasticity, and memory. *Journal of Neuroscience, 27*, 355–365.
Soderling, S. H., Langeberg, L. K., Soderling, J. A., Davee, S. M., Simerly, R., Raber, J., & Scott, J. D. (2003). Loss of WAVE-1 causes sensorimotor retardation and reduced learning and memory in mice. *Proceedings of the National Academy of Sciences of the United States of America, 100*, 1723–1728.
Tolias, K. F., Bikoff, J. B., Burette, A., Paradis, S., Harrar, D., Tavazoie, S., ... Greenberg, M. E. (2005). The Rac1-GEF Tiam1 couples the NMDA receptor to the activity-dependent development of dendritic arbors and spines. *Neuron, 45*, 525–538.
Tolias, K. F., Bikoff, J. B., Kane, C. G., Tolias, C. S., Hu, L., & Greenberg, M. E. (2007). The Rac1 guanine nucleotide exchange factor Tiam1 mediates EphB receptor-dependent dendritic spine development. *Proceedings of the National Academy of Sciences of the United States of America, 104*, 7265–7270.
Yamasaki, N., Maekawa, M., Kobayashi, K., Kajii, Y., Maeda, J., Soma, M., ... Miyakawa, T. (2008). Alpha-CaMKII deficiency causes immature dentate gyrus, a novel candidate endophenotype of psychiatric disorders. *Molecular Brain, 1*, 6.
Yang, N., Higuchi, O., Ohashi, K., Nagata, K., Wada, A., Kangawa, K., ... Mizuno, K. (1998). Cofilin phosphorylation by LIM-kinase 1 and its role in Rac-mediated actin reorganization. *Nature, 393*, 809–812.
Zaqout, S., & Kaindl, A. M. (2016). Golgi-Cox Staining Step by Step. *Frontiers in Neuroanatomy, 10*, 38.
Zhang, H., & Macara, I. G. (2006). The polarity protein PAR-3 and TIAM1 cooperate in dendritic spine morphogenesis. *Nature Cell Biology, 8*, 227–237.